Low Energy Protection System for DC Grids Based on Full Bridge MMC Converters

Dragan Jovcic, *Senior Member IEEE,* Weixing Lin, *Member IEEE,* Samuel Nguefeu, *Member, IEEE, and* Hani Saad, *Member, IEEE*

***Abstract*— This paper studies protection and control methods for a large DC grid based solely on Full Bridge MMC (Modular Multilevel) converters. An initial theoretical study concludes that DC CB energy dissipation will depend on inductance and square of fault current but not on protection operating time. It is proposed to use differential protection because of robust selectivity and also since it operates well with small series inductors. The analysis of DC CB dissipated energy leads to new protection logic design that delays tripping signals until local current reduces to low values. Low speed DC Circuit Breakers with very small inductors are adequate. The design of controllers for MMC converters should be coordinated with DC grid protection and the study derives values for current controller references. The fault recovery time is found to depend on current reference settings at MMC terminals, and optimal values are derived. The conclusions are confirmed using EMTP simulation on a 400kV, 4-MMC DC grid considering two topologies: with 5 overhead lines and with 5 DC cables.**

***Index Terms*—AC-DC power conversion, DC power systems, DC power transmission, HVDC converters, HVDC transmission**

I. Introduction

The development of DC transmission grids would potentially bring numerous benefits because of increased operating flexibility, better utilization of assets and increase in reliability, when compared with the existing 2-termianl HVDC [1]. The grid protection system is one of the fundamental technical challenges.

The vast majority of the DC grid research has been focused on HB (Half Bridge) MMC (Modular Multilevel Converters). The HB MMC DC grid protection has been extensively studied, and most methods can be grouped into fast, local-based [2] and those employing communication signals between terminals [3]. Very good technical advances have been made; nevertheless the total cost of a protection system for a complex DC grid is expected to be high. Very fast and expensive DC CB (Circuit Breakers) based on semiconductors and fast mechanical switches will be required. Also, an unresolved challenge is how to avoid HB MMC converter blocking. The DC grid protection can isolate the faulted DC line very fast, but the current magnitudes will be above (or below but with small margin) blocking threshold for HB MMC converters which impacts reliability of DC grid. Furthermore, the energy dissipation in protection systems will be high [1]. HB MMC HVDC also faces new challenges with overhead lines, because of very frequent DC faults and DC CBs (Circuit Breakers) might be required [4].

In recent years some research has been directed on developing FB (Full Bridge) MMC converters [5]-[9]. FB MMC is immune to DC faults, and it can prevent DC fault propagation either by blocking the converter or by controlling the DC current [1]. The FB-MMC also has the advantages of operation with low DC voltage and the ability to generate higher AC voltage for a given DC voltage limit. Also MMC submodules do not need high-current bypass switches. The cost of FB converter is expected to be around 80% higher while losses might amount to 60% over the HB MMC [10].

The first application of FB MMC HVDC will be with overhead lines, which require frequent DC voltage reduction in order to extinguish DC arc. The German Ultranet FB MMC HVDC project is under construction and several other HVDC projects with overhead lines are under investigation.

The control principles of FB MMC HVDC are more complex than with HB MMC, but studies and performance have been demonstrated on simulation models [7]-[9]. These studies confirm steady-state performance and propose control options for DC faults, but they are concerned solely with 2-terminal HVDC systems. The recent publication [11] examines FB MMC control in DC grids, however no coordination with protection system is provided.

This article studies development of complex DC grids using solely FB MMC converters. The protection system for FB MMC DC grid could potentially be simpler and components could be less expensive since FB MMC terminals can actively manipulate DC currents. However, it is not clear if the protection techniques and DC CBs developed for HB MMC DC Grids are suitable. Indeed, the primary requirement for HB DC Grid protection is rapid operation, which may not be relevant with FB MMC grids. Also, the control methods for MMC under DC faults and during fault recovery should be developed, integrated into normal FB MMC controls and DC grid controls, and coordinated with DC grid protection.

This paper postulates that reduction in energy dissipation should be main requirement with FB MMC DC grid protection design. The significance of energy dissipation, the impact on system performance, costs, and size will all be investigated.

II. DC CB Energy dissipation in DC grids

A. DC grids with HB MMC converters

Unlike the AC CBs and AC transmission grids, the energy dissipation in DC CBs is quite high (it can reach tens of MJ) [12], and it is one of the main technical challenges in the DC

This project is funded by RTE, Paris, France.

D. Jovcic and W. Lin are with the School of Engineering, University of Aberdeen, AB24 3UE, U.K. (d.jovcic@abdn.ac.uk, weixinglin@abdn.ac.uk). S. Nguefeu and H. Saad are with the Réseau de Transport d'Electricité, Paris 92932, France (samuel.nguefeu@rte-france.com, hani.saad@rte-france.com)

grid development. The situation is substantially further complicated if successive DC CB operations are required within a short time, like with grids using overhead lines (OHL), or with some protection methods proposed for cable DC grids (open grid methods). Since energy absorbers need some time period to reduce temperature after receiving a high energy pulse, it is required to install a second (or third) energy bank. The energy dissipation has significant impact on DC CB size, weight and costs.

The energy dissipation in DC CB surge arresters is [12]:

$$E_{dccb} = \int_0^{tc} I_{dc}(t)\,\mathrm{V}_{\mathrm{arr}}(t)dt \tag{1}$$

Where V_{arr} is the arrester voltage, I_{dc} is arrester current and t_c is the fault current suppression time. HB MMC converters require high DC voltage for continued operation, and the DC bus voltage V_{dc} can be assumed constant under DC faults. The arrester voltage is also approximately constant $V_{arr}=3/2V_{dc}$. The fault current suppression time is therefore obtained as:

$$t_c = \frac{2L_{dc}I_p}{V_{dc}} \tag{2}$$

where L_{dc} is the total inductance in the current path, and I_p is the peak DC current, which will be directly proportional to $V_{dc}T_b/L_{dc}$, where T_b is the breaker opening time. Assuming zero load current when the fault occurs, replacing (2) in (1) an approximate expression for DC CB energy dissipation in a constant-voltage HB DC grid is obtained:

$$E_{dccb\_HB} = \frac{3}{2}\frac{V_{dc}^2 T_b^2}{L_{dc}} \tag{3}$$

It is seen that DC CB energy in (3) is crucially dependent on the breaker opening time and the grid voltage. A larger inductor has overall effect to reduce energy dissipation. In a typical system ($V_{dc}=400kV$, $T_b=0.0025s$, $L_{dc}=0.1H$), ignoring line inductance, the energy of around *15MJ* is obtained.

B. DC grid with FB MMC converters

With FB MMC converters, DC voltage can be manipulated in fast manner under DC faults, and considering relatively slow DC grid protection (*10-30ms*), DC bus voltage on all terminals can be assumed to reduce to zero $V_{dc}=0$. The MMC inner current controls will limit current magnitude, and the whole grid becomes constant current system $I_p=const$. Replacing these assumptions, the current suppression time is 1/3 of the value in (2), and replacing in (1), the energy in DC CB in FB DC grids is obtained as:

$$E_{dccb\_FB} = L_{dc}I_p^2 \tag{4}$$

It is clear that the DC CB energies in FB and HB DC grids are much different and the main conclusions from (4) are:

- Energy is crucially dependent on interrupting current,
- Energy increases with inductor size,
- Energy does not depend on the breaker operating time.

Considering the parameters used further in this article ($I_p=450A$, $L_{dc}=0.005H$), the energy of *1.01kJ* is obtained. The above equations are derived to understand the energy dependence on parameters and operating conditions. The accuracy of conclusions are confirmed on digital simulation; however because of simplifying assumptions, these equations cannot give accurate energy values in each DC CB.

III. TEST CIRCUIT

A. Topology

The test system employed is a 4-converter segment of CIGRE B4.57/58 DC grid system [13], which is a stiff bipole, but only one pole is employed for simplicity, as shown in Fig. 1. This system includes a meshed section and a radial line, with large distances (*800km* between MMC1 and MMC3) in order to represent challenging case for protection and control.

Initially all overhead lines are assumed, which are modeled using frequency-dependent distributed model in EMTP [14] and the line data are given in the Appendix. In the last simulation section a case with all DC cables is presented.

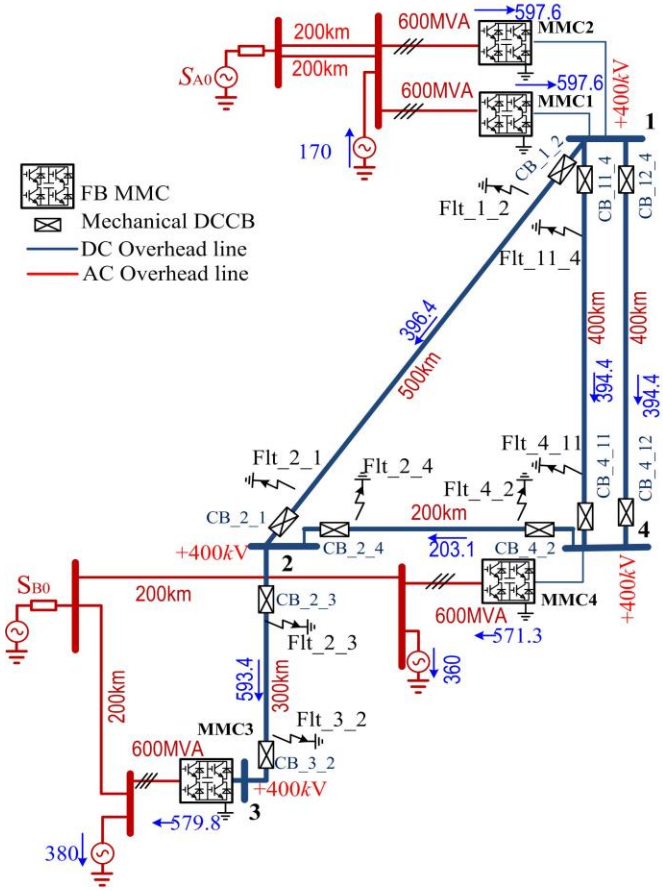

Fig. 1. 4-terminal, 5-line, DC grid test system.

B. Full Bridge MMC

In line with DC grid benchmark [13], all MMC terminals are rated *600MVA*, *400kV*. The average value FB MMC model is used [15], with *1.6kV* rated cell voltage and *250* cells per arm. The MMC energy is *33kJ/MVA*, arm inductance is *0.3pu*, while transformer inductance is *0.18pu*. All cells are assumed of FB type, and this implies that converter can regulate DC voltage in full range $-400kV<V_{dc}<400kV$. A small *0.005H* inductor is placed at each DC connecting point for limiting DC current in case of close-by DC faults.

C. Full Bridge MMC controller

FB MMC has an additional controllability compared with HB MMC which can be exploited to regulate one variable on the DC side [7],[9].

Fig. 2 shows the simplified topology of proposed controller for FB MMC in a DC grid. The control signal M_{dc} is the additional FB MMC control signal which regulates DC current in normal operation. In cascade with the inner DC current regulator, each DC grid terminal includes DC voltage and power control as proposed in [16]. The local power reference P_{DCref} is moderated with P_{disp} signal from the DC grid dispatcher, which manipulates overall DC grid performance.

It is also important that FB MMC employs an arm voltage controller, which is continuously balancing internal MMC energy. Energy balancing may override DC current control in order to prevent dangerous arm voltage levels [7][9].

D. FB MMC control under DC grid faults

There are several options to control FB MMC under faults in a DC grid:

1) *Block FB MMC.*

This is the simplest approach and enables immediate interruption of fault current. On the downside, blocked MMC can not provide reactive power support to the AC grid (STATCOM function). This method is not studied further.

2) *No special control for fault conditions (Protection option I)*

The MMC natural response to DC fault means that DC current reference will hit saturation and each MMC will control local DC current to $I_{dclim}=1.1pu$, as seen in in Fig. 2. The total current feeding the fault I_{fault} will be the sum of all MMC currents from *n* terminals:

$$I_{fault} = \sum_{i=k}^{n} I_{dc\lim k} \tag{5}$$

This total fault current will be shared between the two DC CBs at the ends of the faulted DC line. It is difficult to estimate share of the fault current between the two DC CB, but a conservative estimate is that DC CB current will not exceed:

$$I_{dccb\max} = \sum_{k=1}^{n-1} I_{dc\lim k} \tag{6}$$

Assuming that all MMCs have the same power, the total current feeding the fault will be *1.1n pu*. If a grid is large, this DC CB interrupting current may be large.

Fig. 3 shows the DC grid response for a *Flt_11_4* (zero-impedance fault at line side of *DC CB 11_4*), with the above control method (no protection is active). Fig. 3a) shows that each MMC regulates local DC current to *1.1pu*, but it takes around *50ms* for all currents to settle at the reference values. Fig. 3b) shows that DC voltage response at MMC is very fast, in particular at the terminal MMC1 close to the fault. Fig. 3c) shows that the arm voltage initially increases, but because of energy unbalance between AC and DC sides of each MMC, balancing controller acts on DC current reference to limit arm voltage. This energy balancing is the reason for MMC DC current swings in the first *40ms*. Fig. 3d) shows that the sum of DC CB currents at the faulted line is around *6.6kA*, which is in agreement with (5) (*4x1.1x1.5kA*).

It is seen that DC voltage is close to zero within *10-20ms* but at the remote end MMC3 takes *50-60ms* to reduce DC voltage and multiple oscillatory modes are present. There is clear interest in reducing DC voltage across entire DC grid, since this will imply very low energy dissipation in the DC CB energy absorbers as assumed in deriving (4). This suggests that it may be beneficial to employ slow protection system.

3) *Reduce MMC DC current reference when DC fault condition is detected (Protection option II)*

This is the additional MMC control loop labelled as "Current limiting for DC faults" in Fig. 2. This logic measures only local DC voltage to limit current at $I_{dclim}=I_{dcmin}$ during DC faults, and therefore no grid communication is required.

Reducing currents on each MMC will reduce fault current in DC CBs. The value I_{dcmin} should be low in order to reduce DC CB energy. However it can not be too low since post fault grid recovery would not be possible. On clearing DC fault, this positive I_{dclim} current at each MMC enables line charging and DC voltage increase. When DC voltages rise sufficiently DC voltage controllers will take over naturally and distribute appropriate current references to each terminal.

Fig. 4 shows the DC grid response assuming that DC current is limited to $I_{dclim}=0.15kA$ at each MMC terminal. In Fig. 4 b) it is seen that $I_{dccb\_11\_4}=0.45kA$ while $I_{dccb\_4\_11}=0.15kA$ after *20ms*, which agrees with (5) and (6).

4) *Reduce MMC DC current reference to zero.*

If current is reduced to zero at each MMC terminal, the current at the faulted line would be zero and potentially disconnectors could be used instead of DC CBs. However, because of oscillatory dynamics, it would take much longer time for currents on all lines to settle to zero. Also, once faulted line is disconnected, DC voltage would not recover. It would be necessary for disconnections to communicate to all terminals "fault cleared", in order to begin energisation of DC grid. Because of importance of grid recovery time, this method is not considered further.

E. DC grid controller

A central DC grid dispatcher controller is employed which regulates average DC voltage [16]. This is a slow tertiary

controller which optimizes DC grid operating point and sends power adjustments (P_{disp}) to each terminal with a *20ms* delay.

IV. Protection System

A. Protection logic

There are several options for protection strategy:

1) *ROCOV (Rate of change of voltage) protection.*

This is the fastest method to detect faults and it is reasonably reliable for moderate length DC cables/lines. It is a popular method for HB DC grids [2], but the disadvantages include: requirement for large inductors (over *100mH*) to enable selectivity, and selectivity problems with long/short DC cables, overhead lines and with high impedance faults.

2) *Differential protection*

This is very accurate method, does not require series inductors and works well for high impedance faults on long or

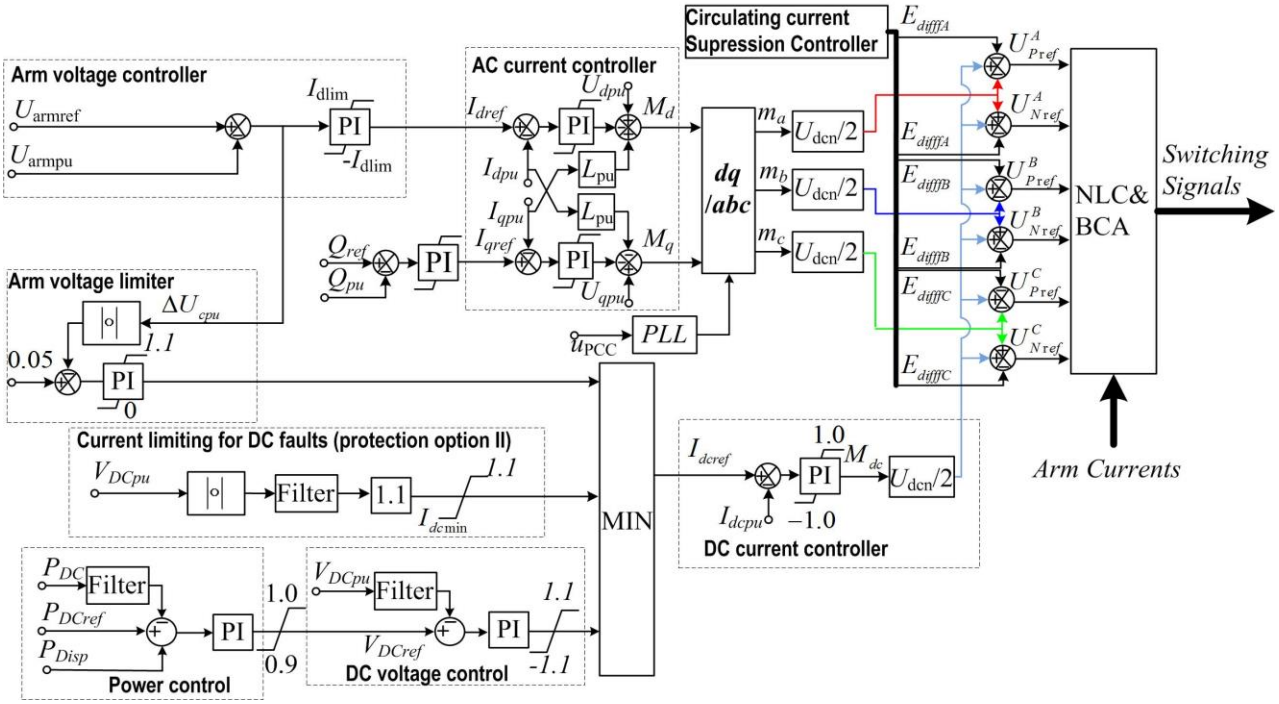

Fig. 2. FB MMC controller.

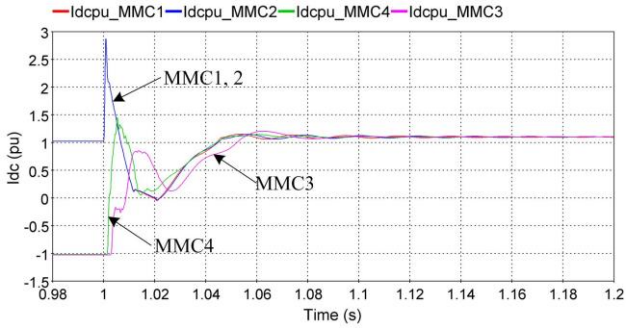

a) MMC DC currents

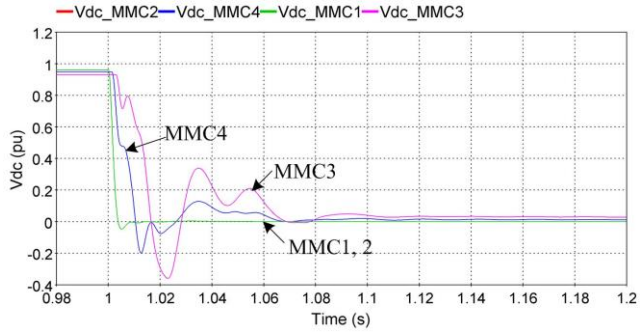

b) MMC DC voltages

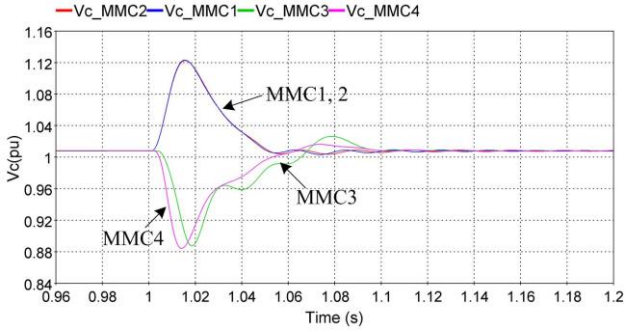

c)MMC cell voltages

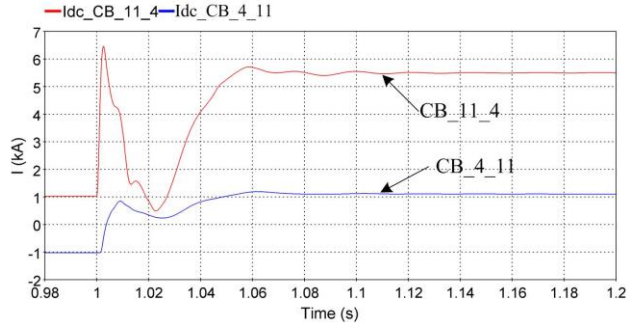

d) Currents on the faulted DC line.

Fig. 3. DC grid response for a fault at FLT 11_4. No protection is active and no MMC current limiting is used.

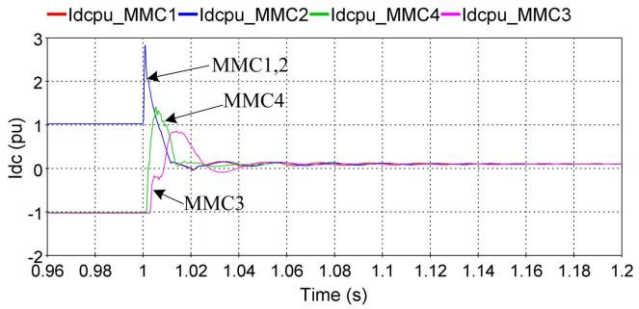

a) MMC DC currents

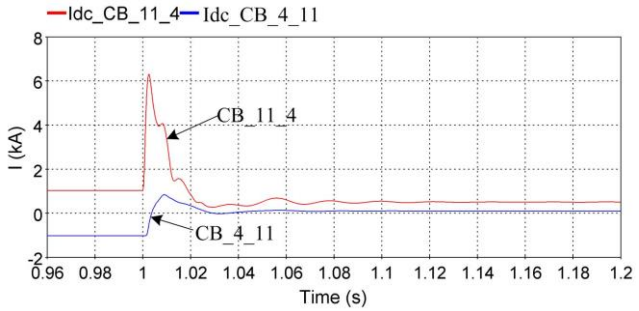

b) Currents on faulted DC line.

Fig. 4. DC grid response for a fault at FLT 11_4. No protection is active. MMC current limiting (*Idcmin=0.1kA*) at all terminals is employed.

short lines [3]. On the downside, it is relatively slow method and reliability is dependent on the communication link between the DC line terminals.

The differential protection is selected for FB DC grid, considering that speed of protection response is not critical. Importantly also, differential protection operates well with very small inductors. According to (4) low inductors will minimizes DC CB energy absorbers, and additionally this improves transient responses.

Fig. 5 shows the protection logic for "*i*" relay on "*ij*" DC line. The topology is similar to the methods in [3], where each relay receives local current measurement I_{dci}, and also current measurement from the remote line end I_{dcj} (via communication link). Since the line lengths are known, and assuming propagation speed of *200km/s*, the delay can be determined. The total time delay of analog-digital conversion and signal processing is assumed to be *20μs* which is added to transmission delay, and Table 1 shows T_{dij} delays used.

Observing Fig. 4 b), and considering responses for other faults, it is concluded that currents on faulted DC lines reduce to steady-state low values in around *20-60ms*, but this time is different for each fault. Differential protection normally operates faster, within *2-5ms* [3]. In order to reduce energy dissipation, it is proposed to include additional logic function labeled "protection option II" in Fig. 5. This logic delays tripping of DC CB until local current drops below I_{dctrip}. This threshold value should be coordinated with the MMC controls, and it is recommended that $I_{dctrip} \geq I_{dccbmax}$ as obtained from (6). Otherwise, there is danger that DC CB will not trip.

3) *Backup protection*

The backup protection against DC CB failure employs similar strategy as for most primary protection methods. It is based on bus-bar level communication with adequate thresholds and time delays [3].

4) *Auto reclosure*

With overhead lines most faults are transient and commonly reclosure is used. However, it is required to allow sufficient time (*300-500ms* for *400kV* systems) for deionization of insulation before line is energized. Since proposed protection operates and system recovers typically within *100ms*, reclosure does not interfere with primary protection.

B. DC circuit breakers

In recent years two main DC CB topologies have become commercially available [12]: hybrid DC CBs with operating time *2-3ms* and mechanical DC CBs with operating time *8-10ms*, and either topology can be employed. Mechanical DC CBs are expected to have substantially lower costs [12], and since operating time has little relevance with energy of FB DC grids as seen in (4), they are selected. It is noted that there are 10 DC CBs in the test system, and the total cost of protection system will have large impact on the overall cost.

The series inductors L_{dc} are universally assumed with DC CBs in HB DC grids for the following 3 reasons:

1. They limit fault current in DC CBs within rating, for the duration of DC CB opening.
2. They prevent DC fault current to reach MMC blocking levels.
3. They enable discrimination between internal and external faults in fast protection methods (like ROCOV).

None of these requirements may apply if DC grid is developed with FB MMC, and therefore small inductors can be used. Inductor size and weight is also very important for offshore installations. For the selected L_{dc}*=0.005H* the weight is around *2.5t* using formulae in [1]. The weight of air core inductors approximately depends on square root of inductance and for inductors with HB DC grids the weight might approach *20t- 30t* [18].

A model for current-injection type mechanical DC CB has been presented in [17], and the model parameters used in this study are shown in Table 2.

V. Simulation Study

A. Study method

A complete system model is developed on EMTP-RV platform and a wide range of zero-impedance faults on each DC line is simulated with two protection options:

- Protection I assumes no current limiting at MMC terminals and immediate DC CB tripping on differential current threshold.
- Protection II assumes that MMC current is limited to I_{dcmin}*=0.1pu (150A)* at each MMC and that DC CB tripping is delayed until local current falls below I_{dctrip}*=0.45kA*. This value is determined using (6) as $I_{dctrip}=3I_{dcmin}$.

The following is monitored:

- Energy at each of the two DC CB at the faulted line,
- Peak current at each of the two DC CBs at faulted line,
- DC grid recovery time, measured when the average dc voltage reaches *0.8pu*.

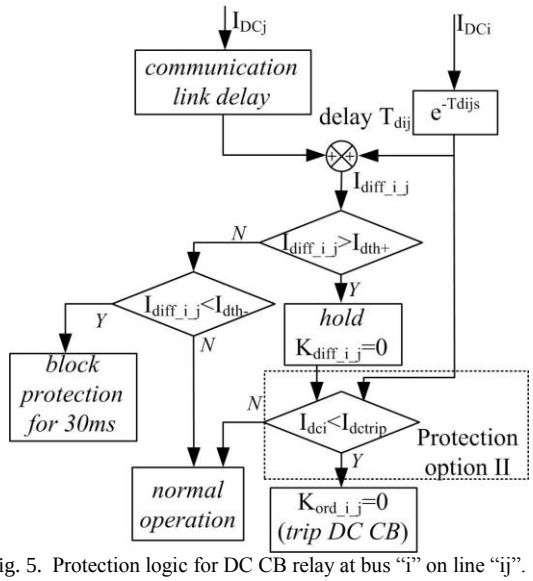

Fig. 5. Protection logic for DC CB relay at bus "i" on line "ij".

Table 1. PROTECTION DELAYS

line	Length (km)	Protection delay T_{dij} (ms)
1_2	500	2.52
11_4	400	2.02
2_3	300	1.52
2_4	200	1.01

Table 2. MECHANICAL DC CB PARAMETERS

Label	Physical Meaning (value)
V_{dcn}	Rated pole-to-ground DC voltage(is *400kV*)
T_{mec}	Contact moving time of the main switch K_{CB} (8*ms*)
T_{LC}	Contact moving time of the resonant switch K_{LC} (0ms)
T_{res}	Operating time of the residual switch S_2. (30ms)
V_{arrn}	Rated voltage of the arrester (304kV)
L_{dc}	Inductance of limiting reactor (0.005H)
L	Inductance of the commutation branch(0.002H)
C	Capacitance of the commutation branch (7.2e-6 F)
I_{mec}	Residual current of the K_{CB} and K_{LC} (300A)
I_{res}	Residual current of the isolator switch (10A)
I_{pk}	Maximum breaking current of the DC CB (16kA).
R_{CH}	Charging resistor. (38Ω)

B. Protection option I

Table 3 shows the results with protection I. The recovery time is fast with *42ms* being the worst case. The peak current in DC CBs is generally lower than expected steady-state values in (6), since DC currents fluctuate in the first *20ms*.

In addition to peak current, inductance in the current path determines fault energy according to (4). Therefore, the DC CB further away from the fault with highest interrupting current potentially dissipates highest energy and study concludes that DC CB 2_3 demands largest energy absorber.

It is interesting to observe that in the worst case the energy dissipation is *18.5MJ* in *CB2_3*, which is very large value and comparable with HB DC grids. The line inductance is quite large (L_{2_3}*=0.28H* from the Appendix) and for the given peak current, formula (4) gives *7.3MJ*. The additional energy is injected from the other lines (lines 1_2 and 2_4) but their current is not fully dissipated by CB2_3 and hence (4) will not give accurate result. The current in the other lines is difficult to determine analytically because of fast MMC controller actions which redirect currents between un-faulted lines.

These studies concluded that protection option I would not bring much (cost) benefit over HB DC grids.

C. Protection option II

Table 4 shows the performance of protection option II. It is remarkable that energy dissipation is extremely low for all fault cases. Similarly as in the previous section, the worst energy dissipation happens for a DC CB connected to radial line with inverter terminal (DC CB_2_3), but the observed energy of *0.37MJ* is very low.

The actual interrupting currents in Table 4 are different from I_{dctrip}*=0.45kA*, because it takes further T_{cb}*=8ms* for DC CB to operate after a trip signal, and current fluctuates in this period. It is recommended that DC CB current rating is substantially larger than I_{dctrip}. Also importantly, it is seen that some interrupting currents are negative, implying that DC CBs should have bidirectional capability.

The fault recovery time is *60-110ms*, which is longer than with protection I, as expected. The authors believe that this clearing time might be acceptable, considering that the critical clearing time for multi-machine AC systems is typically even longer, and as an example it is *200ms-300ms* for the IEEE 39-bus test system [19]. However, further transient studies on large (inter)national systems with multimachine AC grids and DC grids will be required.

The recovery time is found to depend predominately on the minimal current I_{dcmin} in the MMC current limiting loop. Fig. 6 shows results of the study of the worst recovery time (for all faults) versus MMC minimal current limit. Fast recoveries are feasible but at the expense of larger energy requirements for DC CBs. The authors noticed significant deterioration in recovery time while energy dissipation improvement is not substantial for I_{dcmin}*<0.15kA*, and hence I_{dcmin}*=0.15kA* can be recommended.

Table 3. OHL DC GRID PROTECTION I (I_{DCMIN}=1.1PU)

Fault location	Recovery time	Interrupting current (kA)		DC CB energy (MJ)	
		Fault end	Opposite end	Fault end	Opposite end
1_2	40	3.1	0.8	0.2	0.001
2_1	42	6.0	2.6	0.65	0.58
2_3	37	7.2	1.8	3.4	0.001
3_2	22	1.3	5.1	0.002	**18.5**
2_4	35	4.8	4.2	0.7	1.7
4_2	40	1.9	5.0	0.002	0.55
11_4	35	3.0	1.1	0.001	0.002
4_11	40	3.9	0.9	0.026	0.006

Table 4. OHL DC GRID PROTECTION II (I_{DCMIN}=0.1PU)

Fault location	Recovery time (ms)	Interrupting current (kA)		DC CB energy (MJ)	
		Fault end	Opposite end	Fault end	Opposite end
1_2	75	0.3	-0.02	0.0018	0.0017
2_1	62	-1.8	-0.7	0.013	0.022
2_3	70	-1.5	1.8	0.009	0.001
3_2	**110**	-1.5	0.1	0.001	0.37
2_4	65	-0.7	-0.9	0.016	0.016
4_2	65	-0.4	-0.3	0.0001	0.0005
11_4	70	0.3	-0.02	0.017	0.016
4_11	60	-0.06	-0.2	0.0001	0.0004

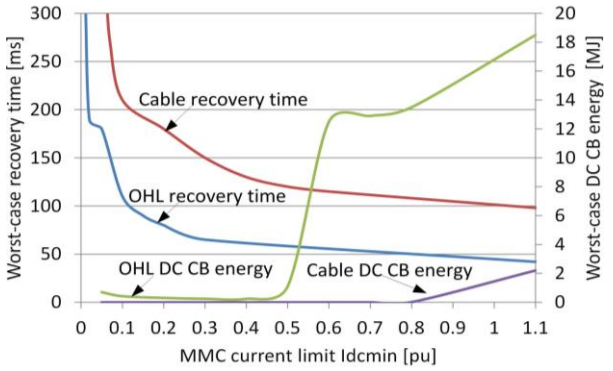

Fig. 6. Recovery time and DC CB energy versus current limit I_{dcmin}.

Fig. 7 shows the *Flt_11_4* simulation with protection II. The DC CBs are tripped around *30ms* after the fault, as seen by the spike on the line currents caused by injection of current from active resonance DC CBs. The DC voltage recovery time is approximately *70ms*. In Fig. 7c) the operation of outer power loops is presented which illustrates that full power (at AC side) is restored in around *300ms* after the fault.

D.Differential current with FB MMC DC Grid

The differential current protection thresholds and selectivity are well understood with HB DC Grids [3], and the authors have firstly developed the protection system for the test system with HB MMC and the same topology as in Fig. 1. The studies show that the same threshold parameters (I_{dth+}*=0.5 and* I_{dth-}*=-0.2* from Fig. 5) can be adopted with the FB MMC DC grid [11].

To illustrate differential protection operation with FB MMC DC grids, Fig. 8 shows the details of the protection operation for *Flt_2_1*, which happens on the longest DC cable representing worst case. The I_{diff} signal from Fig. 5 is also shown. K_{diff} is the differential protection signal from Fig. 5 which becomes K_{diff}*=0* (fault confirmed) around *3ms* after the fault. The conclusions from this study are

- DC current controllers at FB MMC require *5-10ms* to reduce fault current, which marginally decrease differential currents, but this is too slow to interfere with differential protection (assuming lines are not excessively long). Energy discharge form other lines contributes further to increase differential current signal.
- Small inductors are sufficient with FB MMC DC grids, which contribute to slightly increase differential currents.
- The differential protection operates similarly to the case with HB MMC converters.

Fig. 8 also shows operation of the proposed additional protection logic ($K_{ord\_1\_2}$ and $K_{ord\_2\_1}$), which enables each DC CB to trip when local current drops below I_{dctrip}, in order to minimize energy dissipation.

Fig. 9 shows the differential protection operation for a high-impedance (400Ω) fault at *Flt_2_1*. Differential protection generally operates well for high impedance faults, and it is seen that fault is cleared in *20ms*. In this case fault current is low, DC voltage drops marginally to around *0.9pu*, and the MMC current limiting is not activated.

E. Test system with DC cables

The protection method is also analysed with all DC cables employed in the test DC system in Fig. 1. Cable data are given in the Appendix. Table 5 shows the interrupting currents, DC CB energies and recovery times using I_{dcmin}*=0.15kA*. It is seen that the energy dissipation is very low and the interrupting currents are comparable with OHL DC grid. However the

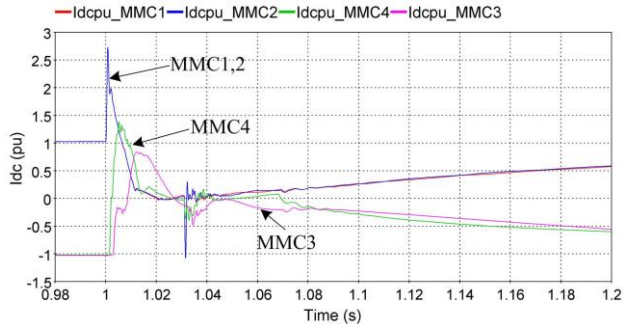

a) MMC DC currents

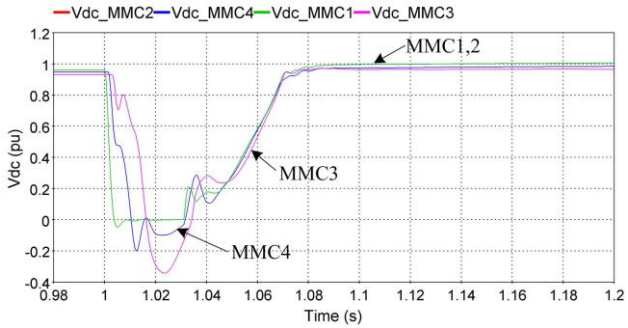

b) MMC DC voltaes

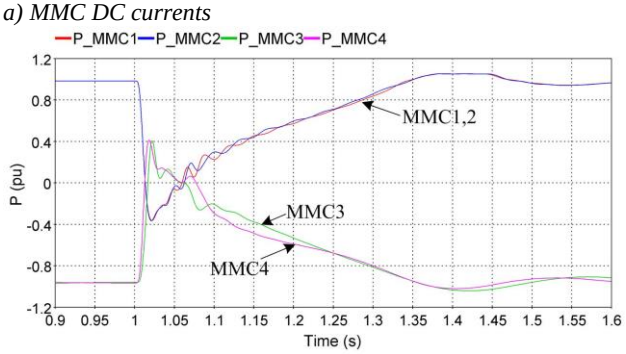

c) AC power of each MMC measured at point of common coupling

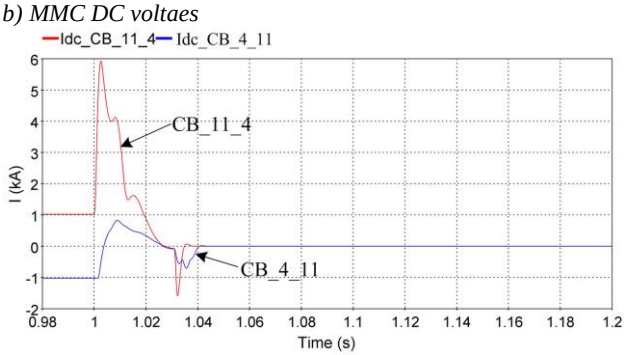

d) DC line curernts

Fig. 7. OHL DC grid response for a fault at FLT 11_4. MMC has fault current limiting (I_{dcmin}=0.15kA) and protection option II is used.

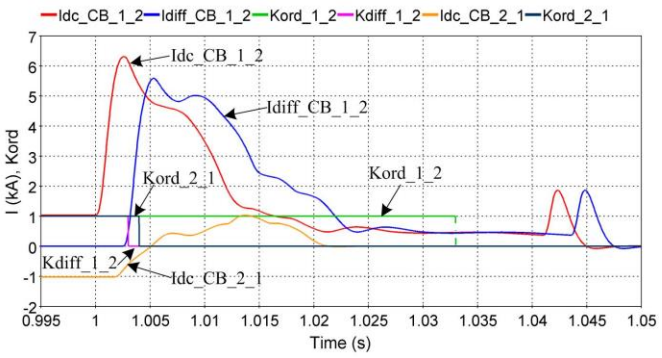

Fig. 8. Protection II operation for a zero impedance fault at FLT 2_1.

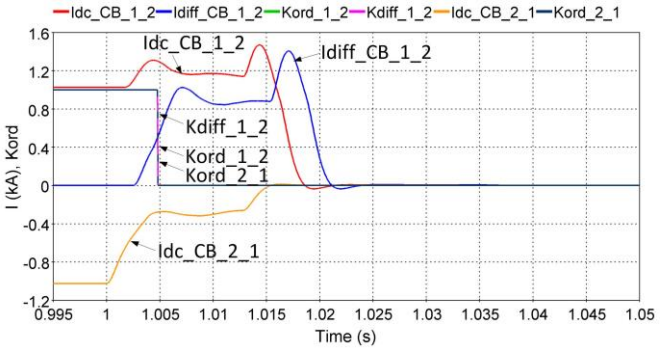

Fig. 9. Protection II operation for a high impedance (*400Ω*) fault at FLT 2_1.

Table 5. CABLE DC GRID. PROTECTION II (I_{DCMIN}=0.1PU)

Fault location	Recovery time (ms)	Interrupting current (kA)		DC CB energy (MJ)	
		Fault end	Opposite end	Fault end	Opposite end
1_2	110	0.2	1	0.00004	0.0002
2_1	115	-0.8	-0.1	0.013	0.00001
2_3	170	-2.3	0.01	0.007	0.005
3_2	**210**	0.01	-1	0.007	0.014
2_4	134	-0.6	-0.8	0.00002	0.015
4_2	132	-0.8	-0.8	0.014	0.013
11_4	122	-2	-1.5	0.00005	0.00003
4_11	130	-1.5	-2.5	0.00008	0.016

recovery time is longer, as it is seen in Fig. 10, which is explained by the considerable values of cable capacitance. Since proposed protection operates by discharging all network energy before line tripping, it is understood that downside is longer post-fault network charge time.

Fig. 6 shows the worst-case recovery time, which indicates that cable system will always have longer recovery time for a given I_{dcmin} (energy dissipation). The worst-case DC CB energy curve in Fig. 6 demonstrates that energy dissipation is lower with cable systems.

VI. CONCLUSION

This paper proposes a low energy protection logic and MMC control method for a DC grid based on FB MMC converters. The theoretical study concluded that DC CB energy dissipation in FB MMC DC grids is proportional to inductance and square of interrupting current but does not depend on the fault clearing time.

It is proposed to use differential protection method, because of robust selectivity and since it does not require large series inductors. Differential protection with FB DC grids is found to operate similarly as with HB DC grids. The study proposes protection logic that delays trip signals until the line currents reduce in order to ensure low energy dissipation.

The protection settings should be coordinated with current limiters at FB MMC terminals, and value of *0.15kA* is found to be optimal current reference for the fault conditions.

The mechanical DC CBs with very small series inductors are recommended and are expected to bring advantages in low costs and size/weight.

The extensive simulation study demonstrates that energy dissipation in DCBs is very low (below *0.4MJ*) while recovery time is normally *60-110ms*. The worst observed recovery time with OHL is *110ms* which might be acceptable, in particular considering cost advantages of the proposed methods.

The studies on DC cable based grid conclude that dissipated energy and interrupting currents are low, but recovery time is longer compared with OHL system.

VII. APPENDIX

Table 6. DC OHL LINE DATA (400KV)

	Conductor	Ground wire
DC resistance [Ω/km]	0.0224	3.65
Outside radius [cm]	2.378	0.475
Horizontal distance [m]	±5	±4.5
Vertical height at tower [m]	30	37
Vertical height at midspan [m]	10	23
Number of conductors in bundle	2	-
Spacing in bundle [cm]	45	-

Table 7. DC CABLE DATA (400KV)

	Conductor	Armour	Sheath
DC resistance [Ω/km]	2.2e-5	27.4e-5	18.1e-5
Inside radius [cm]	0	4.9125	5.6225
Outside radius [cm]	2.5125	5.2225	6.1725
Horizontal distance [m]	±0.25	-	-
Vertical distance (depth) [m]	1.5	-	-
Insulator relative permittivity	2.3	2.3	2.3

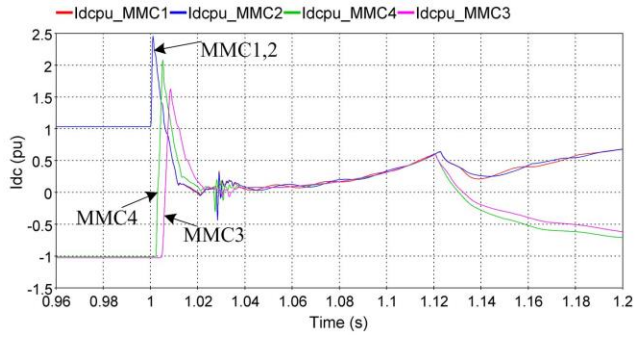

a) MMC DC currents

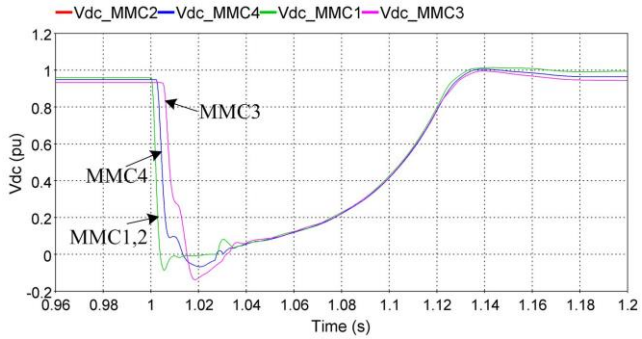

b) MMC DC voltaes

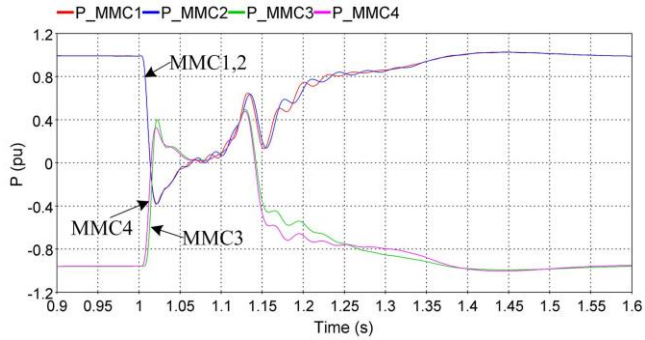

c) AC power of each MMC measured at point of common coupling

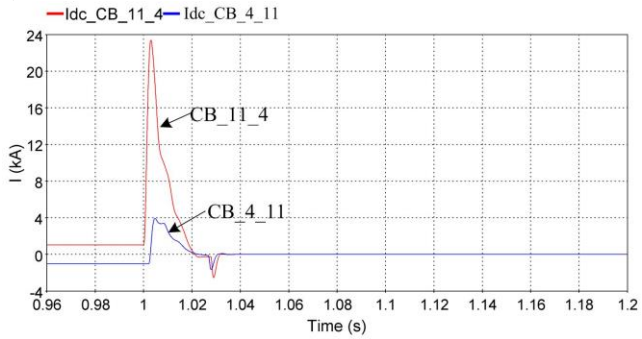

d) DC line curernts

Fig. 10. Cable DC grid response for a fault at FLT 11_4. MMC has fault current limiting (I_{dcmin}=0.15kA) and protection option II is used.

REFERENCES

[1] D Jovcic and K Ahmed "High-Voltage Direct Current Transmission: Converters Systems and DC Grids", Wiley 2015.

[2] J. Sneath, A. Rajapakse, "Fault detection and interruption in an earthed HVDC grid using ROCOV and hybrid DC breakers," IEEE Trans. Power Del., vol. 31, no. 3, pp. 973-981, Jun. 2016.

[3] J. Descloux, B. Raison, J-B. Curis, "Protection strategy for undersea MTDC grids" IEEE PowerTech 2013, Grenoble, France.

[4] T G Magg at all, Zambezi (previously Caprivi) Link HVDC Interconnector: Review of Operational Performance in the First Five Years", CIGRE Paris 2016, B4-108.

[5] W Lin, D Jovcic, S.Nguefeu and H Saad "Full Bridge MMC Converter Optimal Design to HVDC Operational Requirements" IEEE Transactions on Power Delivery, Vol 31, issue 3, 2016, pp1342-1350 ,

[6] R. Zeng, L. Xu, L. Yao, B. W. Williams, "Design and operation of a hybrid modular multilevel converter," *IEEE Trans. Power Electron.*, vol. 30, no. 3, pp. 1137-1146, Mar. 2015.

[7] W.Lin, D. Jovcic, S.Nguefeu and H Saad, "Full Bridge MMC Converter Controller for HVDC Operation in Normal and DC fault Conditions", EE2017, Novi Sad, October 2017

[8] M. Stumpe, P. Ruffing, P. Wagner and A. Schnettler "Adaptive Single-Pole Auto-Reclosing Concept with advanced DC Fault Current Control for Full-Bridge MMC VSC Systems" IEEE transactions on Power delivery" early access, April 2017, DOI: 10.1109/TPWRD.2017.2706361

[9] P. Ruffing, C. Petino, A. Schnettler, "Dynamic Internal Overcurrent Control for undetected DC faults for Modular Multilevel Converters", IET AC and DC Power Transmission, Manchester, UK, Feb. 2017

[10] A Hassanpoor, S Norrga, A Nami, "Loss evaluation for modular multilevel converters with different switching strategies" ICPE-ECCE Asia, 2015,

[11] W.Lin, D. Jovcic, S.Nguefeu and H Saad "Protection of Full Bridge MMC DC grid employing mechanical DC circuit Breakers", IEEE PES GM, Chicago, July 2017.

[12] CIGRE WG A3/B4.38"Technical requirements and specifications of state-of-the-art HVDC switching equipment" *CIGRE technical brochure 683, Paris, April 207*

[13] T K Vrana, Y Yang, D Jovcic, S Dennetière, J Jardini, H Saad, 'The CIGRE B4 DC Grid Test System", ELECTRA issue 270, October 2013, pp 10-19.

[14] J. Mahseredjian, S. Dennetière, L. Dubé, L., B.Khodabakhchian, L. Gérin-Lajoiee, "On a New Approach for the Simulation of Transients in Power Systems," *Electric Power Systems Research*, vol. 77, no. 1, pp. 1514-1520, Sep. 2007.

[15] H. Saad, K. Jacobs, W. Lin, D. Jovcic, "Modelling of MMC including half bridge and full bridge submodules for EMT study," 2016 Power Systems Computation Conference (PSCC), Genoa, Italy, 2016, pp. 1-7.

[16] D.Jovcic and A. Jamshidifar "3-Level cascaded voltage source converters converter controller with dispatcher droop feedback for direct current transmission grids" IET Generation Transmission and Distribution, vol 9 , no. 6 , April 2015, pp. 571-579,

[17] W.Lin, D. Jovcic, S.Nguefeu and H Saad, Modelling of High Power Mechanical DC Circuit breaker APPEEC, 2015, Brisbane, Nov. 2015

[18] E. Kontos, S. Rodrigues, R. Teixeira Pinto and P. Bauer, "Optimization of Limiting Reactors Design for DC Fault Protection of Multi-terminal HVDC Networks", IEEE ECCE 2014, Pp: 5347 – 5354.

[19] M. Eremia and M. Shahidehpour "Handbook of Power System Dynamics", Wiley, 2013.

BIOGRAPHIES

Dragan Jovcic (SM'06, M'00, S'97) obtained a Diploma Engineer degree in Control Engineering from the University of Belgrade, Yugoslavia in 1993 and a Ph.D. degree in Electrical Engineering from the University of Auckland, New Zealand in 1999. He is currently a professor with the University of Aberdeen, Scotland where he has been since 2004. He also worked as a lecturer with University of Ulster, in the period 2000-2004 and as a design Engineer in the New Zealand power industry in the period 1999-2000. His research interests lie in the HVDC, FACTS, and DC grids.

Weixing Lin (M'13, S'11) obtained his Bachelor's degree and PhD degree in electrical engineering in 2008 and 2014 from Huazhong University of Science

and Technology (HUST), Wuhan, China. He was a research fellow at the University of Aberdeen during 2012 to 2016. He is now HVDC director at TBEA Sunoasis. His research interest is different topologies of MMC, simulations on EMPT-RV, dc grids, high power dc-dc converter, high power dc-dc autotransformer.

Samuel Nguefeu (M'04) graduated from École Supérieure d'Electricité (Supélec), Gif-sur-Yvette, France, in 1991. He received the M.A.Sc. and Ph.D. degrees in electrical engineering from Université Pierre et Marie (Paris VI), Paris, France, in 1991 and 1993, respectively. He was a Consultant for two years before joining THOMSON, France, in 1996. From 1999 to 2005, he was with EDF R&D, Clamart, France, in Power Systems and Power Electronics. In 2005, he joined the French Transmission System Operator (Réseau de Transport d'Electricité), where he is currently involved in Flexible AC Transmission Systems and HVDC projects.

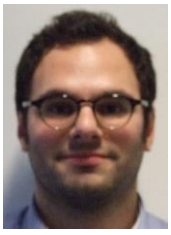

Hani Saad (S'07) received his B.Sc. and Ph.D. degrees in electrical engineering from the École Polytechnique de Montréal in 2007 and 2015, respectively. From 2008 to 2010 he worked at Techimp Spa.and in the Laboratory of Materials Engineering and High Voltages (LIMAT) of the University of Bologna on research and development activities related to partial-discharge diagnostics in power systems. In 2014, he joined the French TSO (Réseau de Transport d'Electricité), where he is currently involved in power system simulation.